J Appl Electrochem (2014) 44:411–418
DOI 10.1007/s10800-013-0643-1

RESEARCH ARTICLE

Facile synthesis of robust free-standing TiO_2 nanotubular membranes for biofiltration applications

Julien Schweicher · Tejal A. Desai

Received: 13 July 2013 / Accepted: 21 October 2013 / Published online: 10 November 2013

Abstract Robust monodisperse nanoporous membranes have a wide range of biotechnological applications, but are often difficult or costly to fabricate. Here, a simple technique is reported to produce free-standing TiO_2 nanotubular membranes with through-hole morphology. It consists of a three-step anodization procedure carried out at room temperature on a Ti foil. The first anodization (1 h at 80 V) is used to pattern the surface of the metallic foil. Then, the second anodization (24 h at 80 V) produces the array of TiO_2 nanotubes that will constitute the final membrane. A higher voltage anodization (3–5 min at 180 V) is finally applied to detach the TiO_2 nanotubular layer from the underlying Ti foil. In order to completely remove the barrier layer that obstructs some pores of the membrane, the latter is etched 2 min in a buffered oxide etch solution. The overall process produces 60-µm-thick TiO_2 nanotubular membranes with tube openings of 110 nm on one side and 73 nm on the other side. The through-hole morphology of these membranes has been verified by performing diffusion experiments with glucose, insulin, and immunoglobulin G where in differences in diffusion rate are observed based on molecular weight. Such biocompatible TiO_2 nanotubular membranes, with controlled pore size and morphology, have broad biotechnological and biomedical applications.

J. Schweicher · T. A. Desai (✉)
Therapeutic Micro and Nanotechnology Laboratory, Department of Bioengineering and Therapeutic Sciences, University of California, San Francisco (UCSF), 1700 4th Street, Box 2520, San Francisco, CA 94158, USA
e-mail: tejal.desai@ucsf.edu

Keywords TiO_2 nanotubes · Membranes · Multi-step anodization · Diffusion of biomolecules · Biofiltration

1 Introduction

TiO_2 nanotubes (NTs) produced by anodization of a Ti foil have increasingly been investigated for biomedical applications due to their excellent interaction with biological tissues [1–5]. Biosensors [1], nanostructured orthopedic and dental implants [1, 6–8], nanostructured vascular stents [1, 9–11], drug delivery vehicles, and drug-eluting coatings [1, 12–15] are typical examples of these applications. Arrays of TiO_2 NTs can also be fabricated as free-standing membranes [16–21] that can be used for biofiltration, e.g., separation of biomolecules, viruses, or cell immunoisolation. Indeed, in addition to being biocompatible, arrays of TiO_2 NTs present excellent characteristics for filtering uses [1, 2] such as: control over pore size and membrane thickness by experimental parameters, narrow pore size distributions, high pore densities, and circular pores that are ideal for blocking flexible biologic molecules.

The first step in the fabrication of a TiO_2 nanotubular membrane is to produce a layer of vertically aligned TiO_2 NTs on a metallic Ti foil by anodization. The influence of the experimental parameters of this process (voltage, current density, duration, electrolyte composition, temperature) has been extensively reviewed elsewhere [1, 2]. TiO_2 NTs with diameters from 15 to 150 nm (mainly controlled by voltage) and lengths from 20 nm to 1,000 µm (mainly controlled by duration) have been produced that way. A total of two anodization steps are usually carried out on the same Ti foil to improve the lateral arrangement of the tubes [22–24]. The first anodization produces a layer of NTs that

is not perfectly ordered and that is removed (e.g., by acid etching or ultrasonication), leaving a dimpled pattern on the Ti foil. The second anodization is then conducted on the textured Ti surface and produces a layer of TiO_2 NTs with improved lateral ordering (close-packed hexagonal arrangement).

TiO_2 NTs produced by anodization have the shape of a test tube: their top end is open and their bottom end is closed (barrier layer in between the tube and the underlying metallic Ti). In order to obtain self-standing TiO_2 nanotubular membranes for flow-through applications, the NTs have to be detached (as an array) from the Ti foil and their bottom ends need to be opened. Liu et al. [21] have published a recent review detailing the numerous techniques developed to tackle these problems. However, the detachment of TiO_2 nanotubular arrays and the opening of their pores still constitute operations that are difficult to realize uniformly in practice, especially for large area membranes.

In this article, we report an easy technique to obtain free-standing membranes of TiO_2 NTs with open ends on both sides. The combination of three anodization steps and a final etch in an acidic solution permits to produce robust membranes that do not curl or crack upon drying. The through-hole morphology of these membranes has been verified by performing diffusion experiments with different biologically relevant molecules.

2 Experimental

2.1 Membrane fabrication

The fabrication technique consists of a three-step anodization procedure carried out at room temperature followed by a final etch step. The starting material is Ti foil (Sigma-Aldrich, 0.25-mm-thick, 99.7 %). A piece of 3 cm × 1.5 cm is cut and ultrasonically cleaned with dilute micro-90 solution (International Products Corporation), then acetone and finally ethanol. The Ti piece is then rinsed with ethanol and dried in nitrogen. The anodization steps are performed in a two-electrode configuration with the Ti foil as working electrode (surface immersed: 2.5 cm × 1.5 cm) and a Pt foil (Alfa Aesar, 0.1-mm-thick, 99.99 %) as counter-electrode. These electrodes are separated by a distance of 7 cm. The electrolyte solution (100–150 ml) consists of ethylene glycol (Sigma-Aldrich) containing 0.3 wt% of NH_4F (Sigma-Aldrich) and 2 vol% of DI H_2O (the experiments are carried out in a Teflon container). The solution is not stirred during any of the anodization steps.

The Ti foil is first pre-anodized in the electrolyte solution at 80 V for 1 h (Agilent E3612A power supply). The produced TiO_2 NTs are detached from the Ti foil by sonicating the sample in a 0.067 vol% HCl aqueous solution (using HCl 50 vol% from LabChem) for 45 min. The resulting patterned Ti surface is then rinsed with DI H_2O and ethanol before being dried in nitrogen.

The second anodization step is also carried out at 80 V but for 24 h (same electrolyte bath as for pre-anodization, same power supply). This step produces the TiO_2 NTs of the final membrane. The Ti/TiO_2 sample is rinsed with water and ethanol before immediate conduction of the next step.

A post-anodization procedure is carried out using a fresh electrolyte solution (of the same composition) and a much higher voltage of 180 V during 3–5 min (Kikusui power supply). The sample is then alternatively rinsed with DI H_2O and ethanol (at least twice) and left drying in air from ethanol. Upon drying, the TiO_2 nanotubular layer detaches from the underlying Ti (a scalpel can be used to assist the separation of the membrane if needed).

The TiO_2 membrane is then soaked for 1 min each side up (total of 2 min) in an aqueous solution of NH_4F 38 wt% and HF 2.4 wt% (buffered oxide etch—BOE—solution 20:1 with surfactant, J.T. Baker). This etching step permits to open all the pores (barrier layer) over the entire bottom side of the sample. The membrane is subsequently rinsed with DI H_2O and ethanol. In order to completely remove the debris layer (nanowires) covering the top side of the sample, the latter is finally sonicated in ethanol for 5 min (VWR Model 75T sonicator) before being rinsed with ethanol and left drying in air. No subsequent annealing step is applied to our TiO_2 nanotubular membranes that thus remain mainly amorphous. If the membranes are handled carefully through the different fabrication stages (plastic tweezers are preferred as compared to metallic ones), it is possible to obtain open-ended areas as large as 2.5 cm × 1.5 cm.

2.2 SEM characterization

The samples have been characterized by field emission-scanning electron microscopy (Zeiss Ultra 55 FE-SEM operated with an acceleration voltage of 2 kV) to obtain morphological and structural information. All specimens have been coated with a 3 nm layer of iridium prior to observation to improve their conductivity.

2.3 Diffusion experiments

Diffusion experiments have been carried out using a custom-made acrylic diffusion chamber (Fig. 1, left). A small piece of a TiO_2 membrane is glued (super glue from Fisher) onto a plastic support containing a 2-mm hole that is entirely covered by the nanotubular membrane (the area available for diffusion is thus 3.14 mm^2). The incorporation of the supported membrane in the diffusion chamber is carried out under DI H_2O to avoid the presence of air bubbles. An elastomer o-ring is used on each side of the

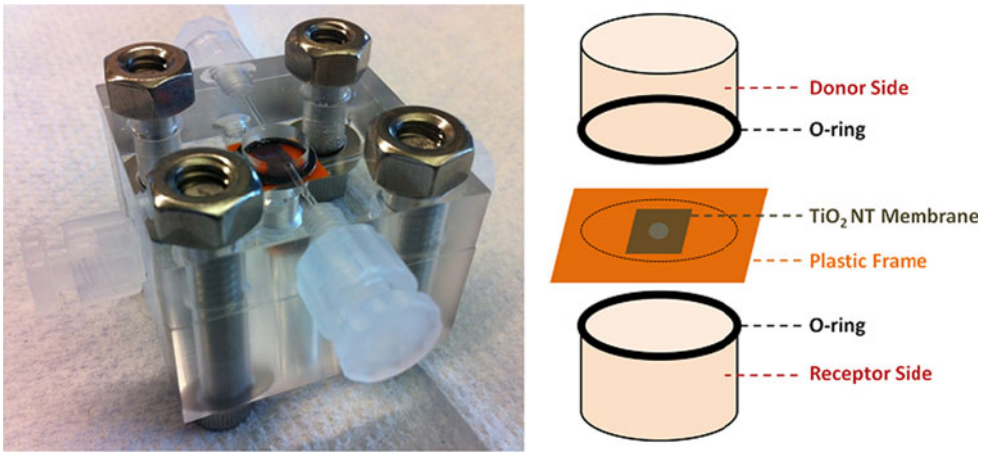

Fig. 1 Photograph of the acrylic diffusion chamber (*left*) and schematic representation of the center part (*right*)

plastic support to prevent any leakage in between donor and receptor compartments (Fig. 1, right). Each compartment presents a volume of 350 µl and is linked to two sampling ports via 1 mm capillaries, allowing easy sampling with a needle and syringe.

All diffusion experiments have been performed at room temperature with the diffusion chamber sitting on a shaking plate. The donor compartment is loaded with a solution of the molecule of interest in DI H_2O, while the receptor compartment contains DI H_2O. The entire volume of the receptor side is removed at determined intervals and replaced by DI H_2O. All the samples are then analyzed as described in the following paragraph.

The diffusion of three biologically relevant molecules has been studied: glucose (D-(+)-Glucose, Sigma-Aldrich, 99.5 %), insulin (Human insulin solution, 10 mg ml^{-1}, Sigma-Aldrich), and immunoglobulin G (IgG) (IgG-FITC from human serum, 20 mg ml^{-1}, Sigma-Aldrich). The starting concentrations (in the donor compartment) of glucose, insulin, and IgG are respectively 3 mg ml^{-1}, 500, and 100 µg ml^{-1}. Glucose analysis is carried out via an enzymatic kit (Glucose (HK) Assay Kit, Sigma-Aldrich) and optical absorbance measurements at 340 nm (SpectraMax 190 spectrophotometer, Molecular Devices). Insulin is analyzed via a micro BCA protein assay kit (Thermo Scientific) and absorbance measurements at 562 nm. IgG is analyzed directly by fluorimetry (FluoroCount fluorimeter, Packard), since it is conjugated to the small fluorescein isothiocyanate (FITC) fluorophore (excitation at 495 nm and emission at 525 nm).

3 Results and discussion

3.1 Membrane fabrication and characterization

At the end of the procedure presented in Sect. 2.1, the TiO_2 nanotubular layer grown during 24 h at 80 V detaches from the underlying Ti foil upon drying from ethanol (Fig. 2, left). A scalpel can be used to assist the separation of the large area membrane if necessary. The produced TiO_2 membrane is mechanically robust and flat (Fig. 2, middle). No curling occurred upon drying in air, as previously reported for other fabrication techniques [17, 18, 25]. As can be seen in the photograph, a thin white layer covers the major part of the Ti foil and is also visible on the upper part of the TiO_2 NT membrane. This intermediate layer grows during the post-anodization step and permits to dislodge the TiO_2 membrane from the underlying Ti (discussed into more details below). An SEM micrograph of the membrane cross section is also provided in Fig. 2, right. Based on this picture, the calculated thickness of the membrane is 60 µm.

The top side of the TiO_2 membrane does not present open end NTs after the triple anodization treatment and the etching step. It is covered by a debris layer of TiO_2 nanowires that have only been slightly attacked by the etching procedure with BOE (Fig. 3, left). However, this debris layer is completely removed after sonication of the membrane in ethanol during 5 min, revealing the open end TiO_2 NTs (Fig. 3, right). The average inner diameter of the tubes is then 110 nm on this side of the membrane. Other experiments have been conducted without the etching step and show that debris nanowires are also completely removed by sonication, proving that etching does not help for this purpose.

On the contrary, the etching step in BOE solution is absolutely necessary to completely open the pores of the bottom side of the membrane (that was in contact with Ti foil prior to its detachment). Indeed, experiments where etching is omitted lead to free-standing membranes with random patches of closed end NTs on the bottom surface as can be seen in Fig. 4A and B. The lighter zones in image A are composed of closed end NTs, whereas the darker areas are constituted by open end tubes. Image B provides a close-up showing two adjacent areas with closed and open end NTs. As mentioned earlier, a thin layer of TiO_2 NTs

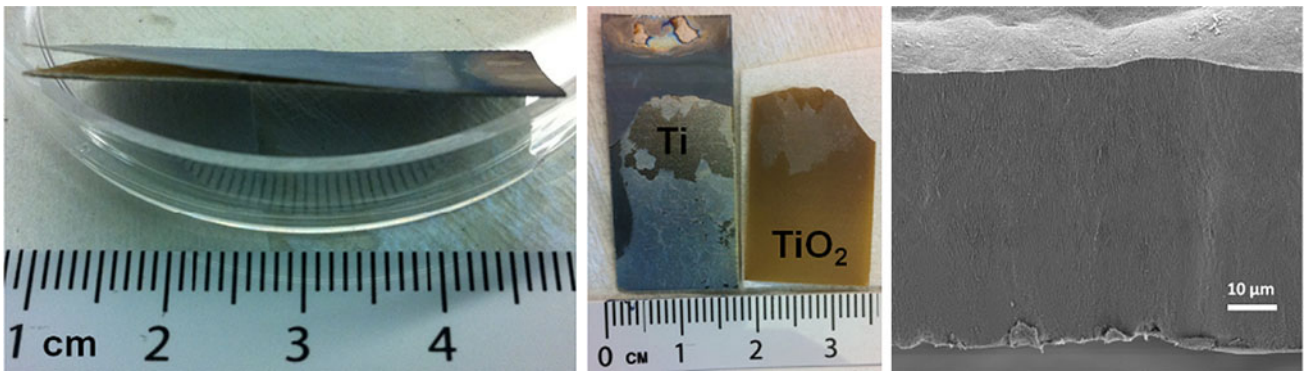

Fig. 2 TiO_2 NT membrane detaching from underlying Ti (*left*), TiO_2 membrane fully detached from Ti (*middle*), and SEM micrograph of TiO_2 membrane cross section (*right*)

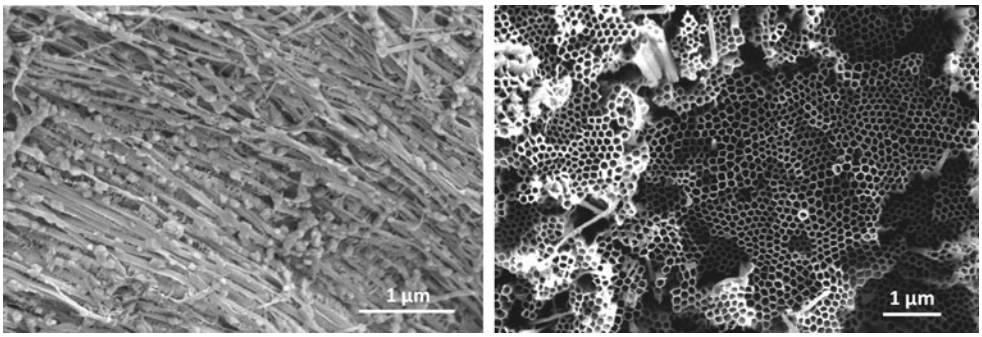

Fig. 3 SEM micrograph of TiO_2 membrane top side after etching in BOE solution (*left*) and after subsequent sonication in ethanol during 5 min (*right*)

grows in between the array of TiO_2 NTs and the underlying Ti foil during the post-anodization step. Since a much higher voltage (180 vs. 80 V before) is used for this third anodization step, the formed NTs have a different diameter than the ones from the layer on top of them. This causes mechanical stress on this upper layer that ultimately detaches as a membrane after drying from ethanol. Some of the membrane NTs caps are torn off during this process and remain on the intermediate layer, thereby producing open end NTs on the bottom side of the TiO_2 membrane. On the contrary, some of these caps remain attached to their original NTs. Another problem is the fact that some parts of the intermediate layer grown during post-anodization can stick to the TiO_2 NT membrane instead of the Ti foil. The middle picture in Fig. 2 highlights this issue on the macroscopic scale and image C in Fig. 4 shows that this problem also exists on the microscopic scale where a chunk of intermediate layer covers an area of open NTs. Image D shows the 600-nm-thick intermediate layer partly covering the underlying Ti foil.

The two issues of incomplete pore opening and pore covering have prompted us to test other experimental conditions (different voltages and durations) for the post-anodization step in order to obtain TiO_2 NT membranes with 100 % open pores on both sides. None of these experiments have led to better results than what has been presented before. This is why a chemical etching step has been envisaged to open the pores and remove the intermediate layer. A buffered oxide etch solution (BOE: NH_4F 38 wt% and HF 2.4 wt% in H_2O) has been used for that purpose. This wet etchant is commonly used in microfabrication to dissolve SiO_2 layers in a controllable manner. The detached TiO_2 membranes are soaked in this solution 1 min each side up (total of 2 min) or 2 min each side up (total of 4 min). The first conditions permit to open 100 % of the closed end NTs and to remove any remaining intermediate layer as can be seen in Fig. 5 that provides two different magnifications of the TiO_2 membrane bottom side after etching (note that the membrane thickness only decreases by a few percents after etching). The tubes present an average inner diameter of 73 nm on this side of the membrane. The second etching conditions do not permit to obtain a clean surface of open NTs because the longer exposition to the etchant creates a lot of debris covering the membrane (not shown).

The complete fabrication process for 60-µm-thick TiO_2 nanotubular membranes with open pores on both sides is summarized schematically in Fig. 6. It is very robust,

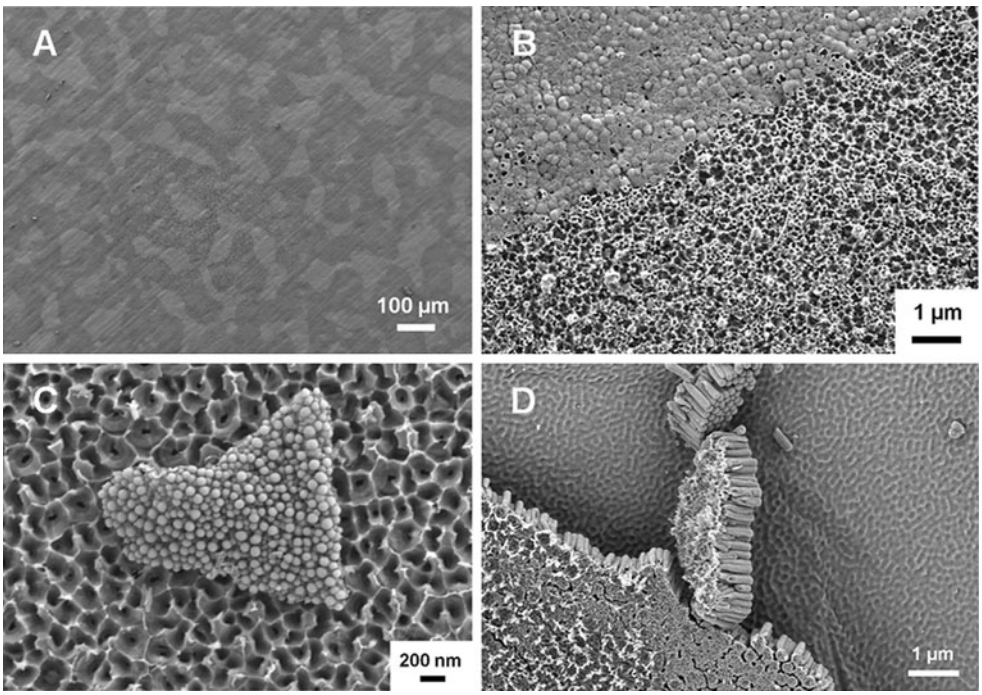

Fig. 4 SEM micrographs of TiO_2 membrane bottom side obtained after three-step anodization and no etching (**A**–**C**), SEM micrograph of the underlying Ti foil partly covered by intermediate layer (**D**)

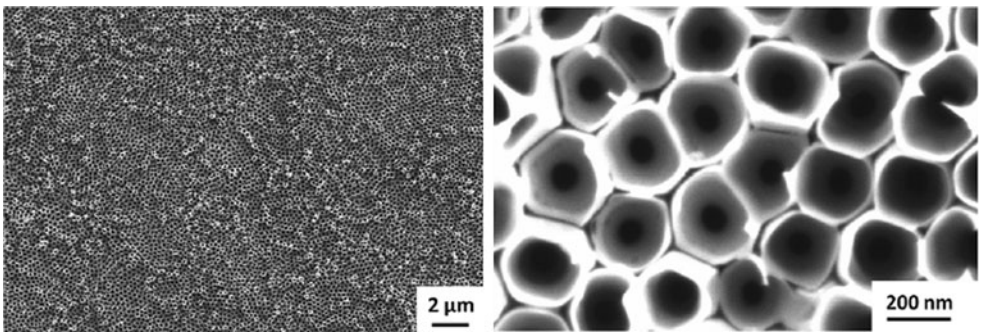

Fig. 5 SEM micrographs of TiO_2 membrane bottom side after three-step anodization and final etching in BOE solution

reproducible, and allows producing quite large area membranes (2.5 cm × 1.5 cm). The post-anodization step induces full detachment of the membrane that already presents some open pores on its bottom side, while its top side is still covered by nanowires. The etching step then permits to completely open the 73 nm pores of the bottom side and remove any remnants of the intermediate layer. Finally, sonication of the membrane in ethanol removes the nanowires covering its top side, revealing NTs with 110 nm pores.

Other authors have used a different (decreased or increased) voltage at the end of the anodization process to detach the TiO_2 membrane from the Ti foil while simultaneously opening the closed bottom ends of the tubes [25–29]. As shown before, we also observe regions of the membrane surface with open pores after increasing the anodization voltage. However, this alternative technique does not result in 100 % open pores over the whole surface without a subsequent etching step. This etching step is thus absolutely necessary to get consistent membranes that could be used for filtration.

Other etchants have been used to open the closed bottom ends of TiO_2 NT arrays (detached by other techniques than voltage decrease/increase in these cases): dilute HF/H_2SO_4 solution [17, 18], NH_4F/H_2SO_4 solution [30], and HF vapors [16]. However, the attack on the TiO_2 membrane is harsher with these etchants, and it is thus more difficult to control it over the whole surface. It is interesting to note that dry etching in a plasma reactor [31, 32] might be as efficient as our wet etching technique to control the opening of the pores, although more expensive.

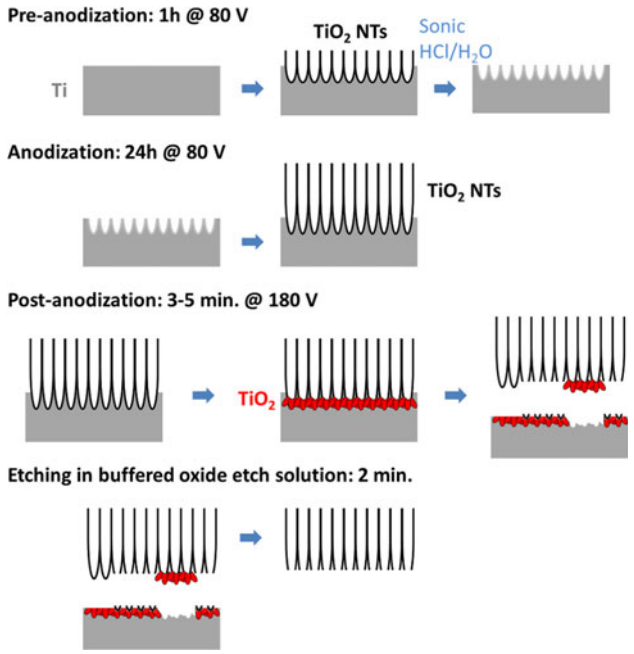

Fig. 6 Overall scheme of the fabrication process for self-standing TiO_2 nanotubular membranes with open ends on both sides

3.2 Diffusion experiments

The diffusion of glucose, insulin, and IgG-FITC through our TiO_2 nanotubular membranes has been studied in the diffusion chamber described in Sect. 2.3. These results are presented in Fig. 7. First of all, it is worth mentioning that all three molecules are able to diffuse through the membranes, thereby proving the through-hole morphology of the NTs. The second important observation is that the diffusion of each of these three molecules follows a zero-order kinetics, since there is a linear relationship between the number of moles diffused and time (see dashed lines in Fig. 7). The linear relationship is clear for glucose and insulin and seems to be valid also for IgG (although more data points are required to confirm this assumption). The diffusion rates are thus independent of concentrations. However, these diffusion rates (determined by the slopes of the lines) are totally different for the test molecules: 38.2 nmol h^{-1} for glucose, 0.03 nmol h^{-1} for insulin, and 0.0002 nmol h^{-1} for IgG. Glucose diffuses about 1,000 times faster than insulin and 200,000 times faster than IgG and insulin diffuses 150 times faster than IgG. These differences can be explained by differences in molar mass (molecular weight) and size for glucose (180 g mol^{-1}; Stokes radius: 0.4 nm) [33], insulin (5,800 g mol^{-1}; 1.35 nm) [34], and IgG (150,000 g mol^{-1}; 5.9 nm) [35, 36]. The correlation between diffusion rate and molar mass is presented in Fig. 8 for the three molecules.

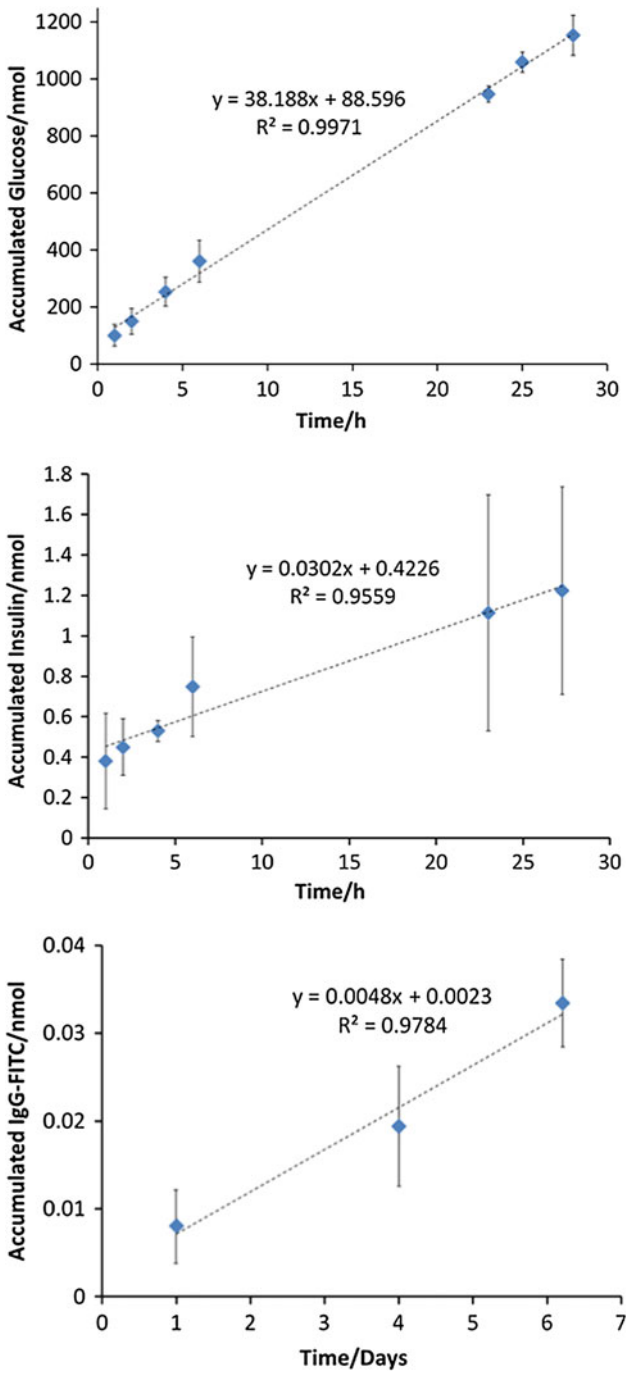

Fig. 7 Diffusion of glucose, insulin, and IgG-FITC through the TiO_2 nanotubular membrane

The demonstrated filtering properties of our biocompatible TiO_2 NT membranes could be used advantageously in biofiltration applications such as viruses' blockage or immunoprotection of transplanted cells. For instance, the immunoisolation of islet or beta cells with TiO_2 NT membranes could potentially lead to a treatment of type 1 diabetes [37], since the diffusion of IgG is largely hindered as compared to glucose and insulin.

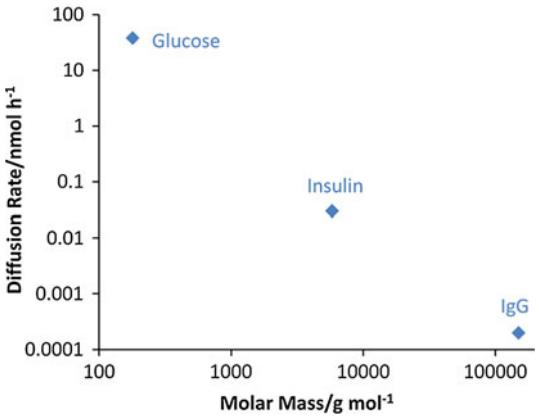

Fig. 8 Diffusion rate of each test molecule as a function of its molar mass (logarithmic scales on both axes)

4 Conclusions

This article reports an easy and reproducible technique to fabricate robust large area TiO_2 nanotubular membranes with open ends on both sides. While the three-step anodization procedure permits to obtain free-standing membranes with some open pores, the final etching step is necessary to open all the pores on the bottom side of the membrane.

The through-hole morphology of these TiO_2 membranes has been verified by diffusion experiments with glucose, insulin, and IgG. The significant difference in diffusion rates for these molecules could lead to interesting biofiltration applications due to the good biocompatibility of titania.

Acknowledgments JS and TAD would like to acknowledge financial support from the Juvenile Diabetes Research Foundation. JS is also grateful for a postdoctoral fellowship (2010–2011) from the King Baudouin Foundation (Belgium) and the Belgian American Educational Foundation. All SEM imaging was performed at the Electron Microscope Facility of the San Francisco State University (SFSU).

References

1. Grimes CA, Mor GK (2009) TiO_2 nanotube arrays—synthesis, properties, and applications. Springer, Dordrecht
2. Roy P, Berger S, Schmuki P (2011) TiO_2 nanotubes: synthesis and applications. Angew Chem Int Ed 50(13):2904–2939. doi:10.1002/anie.201001374
3. Kummer KM, Taylor E, Webster TJ (2012) Biological applications of anodized TiO_2 nanostructures: a review from orthopedic to stent applications. Nanosci Nanotechnol Lett 4(5):483–493. doi:10.1166/nnl.2012.1352
4. Tan AW, Pingguan-Murphy B, Ahmad R, Akbar SA (2012) Review of titania nanotubes: fabrication and cellular response. Ceram Int 38(6):4421–4435. doi:10.1016/j.ceramint.2012.03.002
5. Ainslie KM, Tao SL, Popat KC, Daniels H, Hardev V, Grimes CA, Desai TA (2009) In vitro inflammatory response of nanostructured titania, silicon oxide, and polycaprolactone. J Biomed Mater Res A 91A(3):647–655. doi:10.1002/jbm.a.32262
6. Oh S-H, Finones RR, Daraio C, Chen L-H, Jin S (2005) Growth of nano-scale hydroxyapatite using chemically treated titanium oxide nanotubes. Biomaterials 26(24):4938–4943. doi:10.1016/j.biomaterials.2005.01.048
7. Brammer KS, Frandsen CJ, Jin S (2012) TiO_2 nanotubes for bone regeneration. Trends Biotechnol 30(6):315–322. doi:10.1016/j.tibtech.2012.02.005
8. Minagar S, Berndt CC, Wang J, Ivanova E, Wen CA (2012) Review of the application of anodization for the fabrication of nanotubes on metal implant surfaces. Acta Biomater 8(8):2875–2888. doi:10.1016/j.actbio.2012.04.005
9. Brammer KS, Oh S, Gallagher JO, Jin S (2008) Enhanced cellular mobility guided by TiO_2 nanotube surfaces. Nano Lett 8(3):786–793. doi:10.1021/nl072572o
10. Peng L, Eltgroth ML, LaTempa TJ, Grimes CA, Desai TA (2009) The effect of TiO_2 nanotubes on endothelial function and smooth muscle proliferation. Biomaterials 30(7):1268–1272. http://www.sciencedirect.com/science/article/pii/S0142961208008818. Accessed 14 Oct 2013
11. Peng L, Barczak AJ, Barbeau RA, Xiao Y, LaTempa TJ, Grimes CA, Desai TA (2009) Whole genome expression analysis reveals differential effects of TiO_2 nanotubes on vascular cells. Nano Lett 10(1):143–148. doi:10.1021/nl903043z
12. Popat KC, Eltgroth M, LaTempa TJ, Grimes CA, Desai TA (2007) Decreased Staphylococcus epidermis adhesion and increased osteoblast functionality on antibiotic-loaded titania nanotubes. Biomaterials 28(32):4880–4888. doi:10.1016/j.biomaterials.2007.07.037
13. Popat KC, Eltgroth M, LaTempa TJ, Grimes CA, Desai TA (2007) Titania nanotubes: a novel platform for drug-eluting coatings for medical implants? Small 3(11):1878–1881. doi:10.1002/smll.200700412
14. Peng L, Mendelsohn AD, LaTempa TJ, Yoriya S, Grimes CA, Desai TA (2009) Long-term small molecule and protein elution from TiO_2 nanotubes. Nano Lett 9(5):1932–1936. doi:10.1021/nl9001052
15. Losic D, Simovic S (2009) Self-ordered nanopore and nanotube platforms for drug delivery applications. Expert Opin Drug Deliv 6(12):1363–1381. doi:10.1517/17425240903300857
16. Albu SP, Ghicov A, Macak JM, Hahn R, Schmuki P (2007) Self-organized, free-standing TiO_2 nanotube membrane for flow-through photocatalytic applications. Nano Lett 7(5):1286–1289. doi:10.1021/nl070264k
17. Paulose M, Prakasam HE, Varghese OK, Peng L, Popat KC, Mor GK, Desai TA, Grimes CA (2007) TiO_2 nanotube arrays of 1000 μm length by anodization of titanium foil: phenol red diffusion. J Phys Chem C 111(41):14992–14997. doi:10.1021/jp075258r
18. Paulose M, Peng L, Popat KC, Varghese OK, LaTempa TJ, Bao N, Desai TA, Grimes CA (2008) Fabrication of mechanically robust, large area, polycrystalline nanotubular/porous TiO_2 membranes. J Membr Sci 319(1–2):199–205. doi:10.1016/j.memsci.2008.03.050
19. Albu SP, Ghicov A, Berger S, Jha H, Schmuki P (2010) TiO_2 nanotube layers: flexible and electrically active flow-through membranes. Electrochem Commun 12(10):1352–1355. doi:10.1016/j.elecom.2010.07.018
20. Roy P, Dey T, Lee K, Kim D, Fabry B, Schmuki P (2010) Size-selective separation of macromolecules by nanochannel titania membrane with self-cleaning (declogging) ability. J Am Chem Soc 132(23):7893–7895. doi:10.1021/ja102712j
21. Liu G, Wang K, Hoivik N, Jakobsen H (2012) Progress on free-standing and flow-through TiO_2 nanotube membranes. Sol

Energy Mater Sol Cells 98:24–38. doi:10.1016/j.solmat.2011.11.004
22. Macak JM, Albu SP, Schmuki P (2007) Towards ideal hexagonal self-ordering of TiO_2 nanotubes. Phys Status Solidi 1(5):181–183. doi:10.1002/pssr.200701148
23. Zhang G, Huang H, Zhang Y, Chan HLW, Zhou L (2007) Highly ordered nanoporous TiO_2 and its photocatalytic properties. Electrochem Commun 9(12):2854–2858. http://www.sciencedirect.com/science/article/pii/S1388248107004079. Accessed 14 Oct 2013
24. Ali G, Chen C, Yoo S, Kum J, Cho S (2011) Fabrication of complete titania nanoporous structures via electrochemical anodization of Ti. Nanoscale Res Lett 6(1):332. http://www.nanoscalereslett.com/content/6/1/332. Accessed 14 Oct 2013
25. Wang D, Liu L (2010) Continuous fabrication of free-standing TiO_2 nanotube array membranes with controllable morphology for depositing interdigitated heterojunctions. Chem Mater 22(24):6656–6664. doi:10.1021/cm102622x
26. Kant K, Losic D (2009) A simple approach for synthesis of TiO_2 nanotubes with through-hole morphology. Phys Status Solidi 3(5):139–141. doi:10.1002/pssr.200903087
27. Li S, Zhang G (2010) One-step realization of open-ended TiO_2 nanotube arrays by transition of the anodizing voltage. J Ceram Soc Jpn 118(4):291–294. doi:10.2109/jcersj2.118.291
28. Jo Y, Jung I, Lee I, Choi J, Tak Y (2010) Fabrication of through-hole TiO_2 nanotubes by potential shock. Electrochem Commun 12(5):616–619. doi:10.1016/j.elecom.2010.02.013
29. Liu G, Hoivik N, Wang K, Jakobsen H (2011) A voltage-dependent investigation on detachment process for free-standing crystalline TiO2 nanotube membranes. J Mater Sci 46(24):7931–7935. doi:10.1007/s10853-011-5927-4
30. Fang D, Huang K, Liu S, Luo Z, Qing X, Zhang Q (2010) High-density $NiTiO_3/TiO_2$ nanotubes synthesized through sol-gel method using well-ordered TiO_2 membranes as template. J Alloys Compd 498(1):37–41. http://www.sciencedirect.com/science/article/pii/S092583881000410X. Accessed 14 Oct 2013
31. Zhu B, Li J, Chen Q, Cao R-G, Li J, Xu D (2010) Artificial, switchable K^+-gated ion channels based on flow-through titania-nanotube arrays. Phys Chem Chem Phys 12(34):9989–9992. doi:10.1039/B925961A
32. Li L-L, Chen Y-J, Wu H-P, Wang NS, Diau EW-G (2011) Detachment and transfer of ordered TiO_2 nanotube arrays for front-illuminated dye-sensitized solar cells. Energy Environ Sci 4(9):3420–3425. doi:10.1039/C0EE00474J
33. Pappenheimer JR, Renkin EM, Borrero LM (1951) Filtration, diffusion and molecular sieving through peripheral capillary membranes: a contribution to the pore theory of capillary permeability. Am J Physiol 167(1):13–46. http://ajplegacy.physiology.org/content/167/1/13. Accessed 14 Oct 2013
34. Oliva A, Fariña J, Llabrés M (2000) Development of two high-performance liquid chromatographic methods for the analysis and characterization of insulin and its degradation products in pharmaceutical preparations. J Chrom B 749(1):25–34. doi:10.1016/S0378-4347(00)00374-1
35. Leoni L, Desai TA (2004) Micromachined biocapsules for cell-based sensing and delivery. Adv Drug Deliv Rev 56(2):211–229. doi:10.1016/j.addr.2003.08.014
36. Kang J, Erdodi G, Kennedy JP (2007) Development of two high-performance liquid chromatographic methods for the analysis and characterization of insulin and its degradation products in pharmaceutical preparations. J Polym Sci A 45(18):4276–4283. doi:10.1002/pola.22170
37. Schweicher J, Nyitray C, Desai TA (2014) Membranes to achieve immunoprotection of transplanted islets. Front Biosci (accepted)